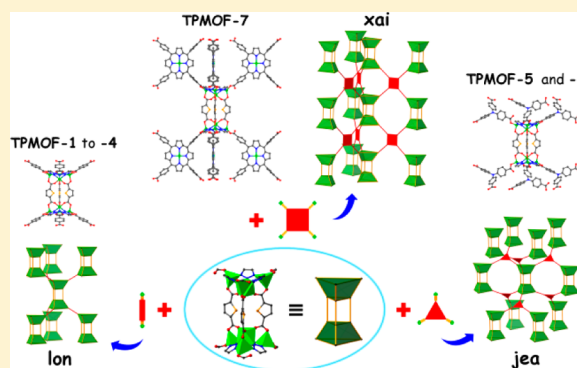


Derivation and Decoration of Nets with Trigonal-Prismatic Nodes: A Unique Route to Reticular Synthesis of Metal–Organic Frameworks

Jun-Sheng Qin,^{‡,§} Dong-Ying Du,[§] Mian Li,[¶] Xi-Zhen Lian,[‡] Long-Zhang Dong,[†] Mathieu Bosch,[‡] Zhong-Min Su,[§] Qiang Zhang,[‡] Shun-Li Li,[†] Ya-Qian Lan,^{*,†,§} Shuai Yuan,[‡] and Hong-Cai Zhou^{*,‡}[†]School of Chemistry and Materials Science, Nanjing Normal University, Nanjing 210023, P. R. China[‡]Department of Chemistry, Texas A&M University, College Station, Texas 77843-3255, United States[§]Department of Chemistry, Northeast Normal University, Changchun 130024, P. R. China[¶]Department of Chemistry, Shantou University, Guangdong 515063, P. R. China

S Supporting Information

ABSTRACT: Quests for advanced functionalities in metal–organic frameworks (MOFs) inevitably encounter increasing complexity in their tailored framework architectures, accompanied by heightened challenges with their geometric design. In this paper, we demonstrate the feasibility of rationally exploiting topological prediction as a blueprint for predesigned MOFs. A new triangular frusta secondary building unit (SBU), $\{Zn_4(tz)_3\}$, was bridged by three TDC²⁻ fragments to initially form a trigonal prismatic node, $\{Zn_8(tz)_6(TDC)_3\}$ (Htz = 1H-1,2,3-triazole and H₂TDC = 2,5-thiophenedicarboxylic acid). Furthermore, the trigonal prism unit can be considered as a double SBU derived from triply bound triangular frusta. By considering theoretical derived nets for linking this trigonal-prismatic node with ditopic, tritopic, and tetratopic linkers, we have synthesized and characterized a new family of MOFs that adopt the decorated **lon**, **jea**, and **xai** nets, respectively. Pore sizes have also been successively increased within TPMOF-*n* family, which facilitates heterogeneous biomimetic catalysis with Fe–porphyrin-based TPMOF-7 as a catalyst.



■ INTRODUCTION

Research investigating metal–organic frameworks (MOFs), also known as porous coordination polymers (PCPs) or porous coordination networks (PCNs), has developed rapidly in the fields of chemistry and material science,¹ largely owing to their underlying topologies in relation to designed synthesis² and the upsurge of applications in gas storage and separation,³ sensing,⁴ catalysis,⁵ biomimicry,⁶ and so on.⁷ As a class of crystalline porous material, a unique aspect of MOFs emerges with the network-based approach, termed *reticular synthesis* by Yaghi et al. and developed by several groups of researchers,^{1a,2d,8} in order to target tailored pore sizes, shapes, and tunable surface properties. The keys to implementing such an approach may include: (i) knowledge of possible periodic nets underlying outcomes of developing reticular synthesis approaches;^{2,9} (ii) a library of well-established metal clusters, known as secondary building units (SBUs), which serve as predefined local geometric nodes;^{8c,10} and (iii) mastery of ligand design and systematic control of the kinetics and thermodynamics of MOF crystal growth.¹¹

In the development of MOF chemistry, the identification of several metal cluster SBUs readily reproducible during MOF growth has led to the continual discovery of new materials.^{9–12} For instance, metal–carboxylate clusters encoded with geo-

metrical information on 4-coordinated (4-c) square, 6-c trigonal-prism, 6-c octahedron, and 12-c cuboctahedron (Figure S1a–d) have been assembled into several iconic MOFs, known as HKUST-1,^{12a} MIL-100/101,^{12b,c} MOF-5,^{12d} and UiO-66,^{12e} respectively. Recently, some polyhedral and cage-like building blocks with high symmetry (Figure S1e–j) have been considered to constitute super SBUs for describing the framework's underlying topology.^{10b,d,13–15} Among them, trigonal-prismatic building blocks with lower symmetry and related networks are of special interest, both mathematically and chemically, perhaps due to the unexpected topology (**moö/mtn**) and ultrahigh porosity of MIL-100/101^{12b,c} and PCN-332/333,^{12f} which can even accommodate enzymes. Among recent research, Zaworotko et al. have performed a series of prominent studies on $[Cr_3(\mu_3-O)(isonic)_6]^+$ unit (isonic = pyridine-4-carboxylate, Figure S1f), a chemically decorated trigonal-prismatic 6-coordinated node (Figure S1b).¹⁴ O'Keeffe and co-workers have considered the theoretical possibilities of connecting trigonal prisms with ditopic, tritopic, and tetratopic linkers in the most symmetrical ways, thereby giving **acs**, **sit**, and **stp** nets, respectively.^{2f,16} However, MOFs with relevant

Received: January 30, 2016

Published: April 5, 2016



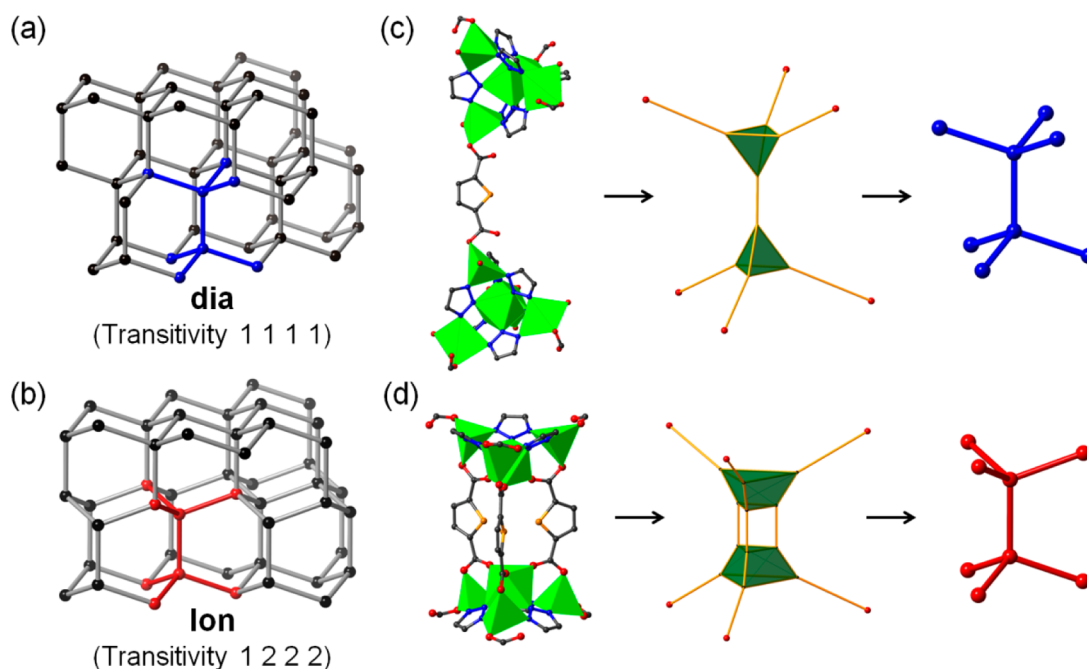


Figure 1. (a) Deconstruction of TMOF into the diamond (dia) net and (b) TPMOF-1 into the lonsdaleite (lon) net. The fragments outlined in blue and red show the distinct local conformations between the two basic nets. (c) Two $\{Zn_5(tz)_6\}$ units linked by one TDC^{2-} fragment in TMOF, which can be deconstructed into two linked tetrahedra (in dark green), and further abstracted into nodes (in blue) connected in a staggered conformation similar to that in dia. (d) Two $\{Zn_4(tz)_3\}$ units linked by three TDC^{2-} fragments in TPMOF-1, deconstructed into two triangular frusta (in dark green) joined by three ditopic linkers and further deconstructed into nodes (in red) connected in an eclipsed conformation in lon. Color codes for atoms: Zn polyhedra, green; O, red; N, blue; C, black; S, yellow; H, omitted.

topology remain largely unexplored, and most of those that have been explored were constructed on the basis of $\{M_3(\mu_3-O)(CO_2)_6\}$ clusters ($M = Cr$ or Fe , Figure S1b).^{10e,14a,17} To date, a MOF system that includes trigonal-prismatic or related SBUs connecting with ditopic, tritopic, and tetratopic organic linkers has not yet been simultaneously established, meaning that the rational route to the reticular synthesis of expected MOFs remains unfinished.

Topical MOF research embraces a trend of “heterogeneity within order”,^{1f,8h} which underscores the increased complexity engineered into the backbones or pores of targeted MOFs. Researchers have successfully demonstrated that the introduction of two types of ligands with different shapes (e.g., a ditopic one and a tritopic one) is an effective route to achieve ultra high porosity, exemplified by the cases of UCM-1 to -5,^{18a-c} DUT-6,^{18d} MOF-205/210,^{18e} NENU-511 to -514,^{18f} MUF-7/77^{19a,b} and UCM-10 to -12.^{19c} Accordingly, a topological design with respect to manifestation of “order out of complexity” and the further experimental realization of such isorecticular series are in great demand.

In our present contribution, we report the discovery of a novel type of triangular frusta SBU, $\{Zn_4(tz)_3\}$, which was further bridged by three TDC^{2-} fragments to initially generate a trigonal prismatic node, $\{Zn_8(tz)_6(TDC)_3\}$ ($Htz = 1H$ -1,2,3-triazole and $H_2TDC = 2,5$ -thiophenedicarboxylic acid) in TPMOF-1 (TPMOF meaning trigonal-prism-derived MOF). Furthermore, the trigonal prism unit can be considered as a double SBU originated from triply bound triangular frusta, and the reticulation of this double SBU connecting with ditopic, tritopic, and tetratopic linkers into periodic nets has been achieved through the rational topological design. We prepared a new family of isorecticular MOFs, TPMOF-2 to -4 with ditopic linkers, TPMOF-5 and -6 with tritopic linkers, and TPMOF-7

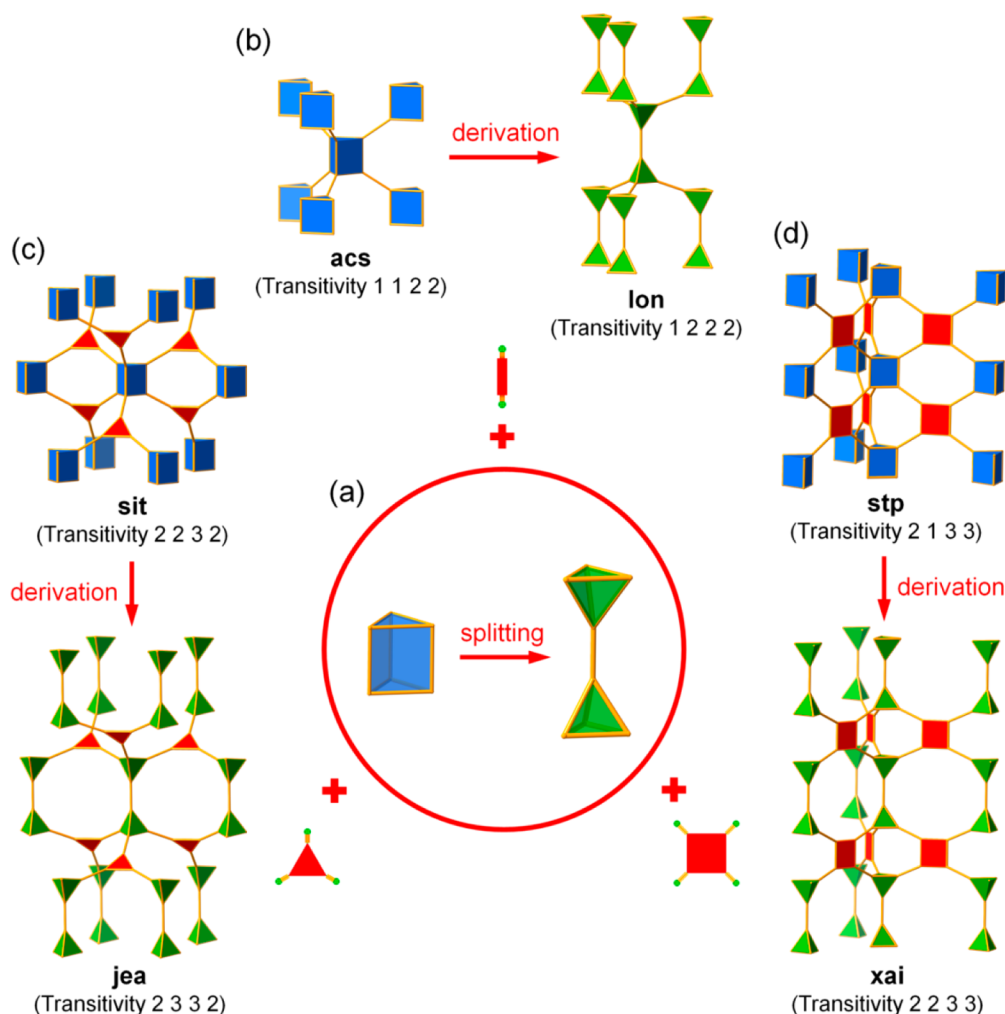
with tetratopic metal–porphyrin-based linker, which exhibits high activity as a heterogeneous biomimetic catalyst.

RESULTS AND DISCUSSION

Realization of Triply Bound Triangular Frusta SBU. In previous work, a type of tetrahedral pentanuclear metal cluster, M_5L_6 ($M = Zn, Cu, Co, Ni, Mn, Fe$, or Mg , $L = 1,2,3$ -triazolate or benzotriazolate) was discovered (Figure S1e) that acted as an SBU or precursor to yield a family of microporous 3D frameworks.^{13a-e} Despite variations on the nature (metal or organic fragment), connection (ditopic or tetratopic), and length of the linkers, the underlying topology of the resulting MOFs is always the diamond (dia) net (Figure 1a). This outcome of the reticular synthesis is not surprising, for the dia net is most commonly observed for MOFs containing tetrahedral nodes, as verified by both network theory and data statistics.^{1a,2d}

Recently, we identified a related tetranuclear zinc SBU, $\{Zn_4(dttz)_6\}$ ($H_3dttz = 4,5$ -di(1*H*-tetrazol-5-yl)-2*H*-1,2,3-triazole), in an anionic framework (IFMC-2).^{13f} Interestingly, a single metal site at the vertex of the aforementioned tetrahedral M_5L_6 cluster was missing, thus yielding a triangular frustum (i.e., singly truncated tetrahedron, Figure S1g). The formation of such a SBU is highly unusual,^{13g} given its mostly unsymmetrical configuration even less regular than C_3 trigonal-prismatic SBU and the anisotropic truncation of the T_d node. SBUs with low symmetry are important in MOF chemistry since they challenge targeted synthesis and facilitate the route to network diversity and high porosity (e.g., MIL-100/101,^{12b,c} PCN-332/333,^{12f} and PCN-777²⁰). It should be noted that similar triangular frustum shaped $M_4(bta)_3$ ($M = Zn$ or Cd/Na , $bta =$ benzotriazolate) is encountered in literature sporadically,^{13g,h} but the systematic study is lacking.

Scheme 1. Theoretical Nets in the RCSR Database Based on Trigonal Prisms (in Blue) Connected by Ditopic, Tritopic, or Tetratopic Linkers (in Red) and Their Derived Nets Obtained by Splitting One Trigonal Prism into Two Linked Tetrahedra (in Green)^a



^a(a) Splitting the trigonal prism into a pair of linked tetrahedra, (b) the ditopic linker with **lon** derived from **acs**, (c) the tritopic linker with **jea** derived from **sit**, and (d) the tetratopic linker with **xai** derived from **stp**. All nets are shown in augmented forms, and the four-digit numbers in parentheses represent the transitivity of basic (i.e., unaugmented) nets.

To study functional multicomponent MOFs, we conducted reticular synthesis containing zinc ions, Htz, and an angular (V-shaped) ditopic linker, H₂TDC. After fine-tuning the reaction conditions, two crystalline products were separately yielded (see [Experimental Section](#)). The first MOF, formulated as [Zn₅(tz)₆(DMF)₄(TDC)₂] (**TMOF**, tetrahedron-derived MOF), crystallizes in the $I\bar{4}2d$ space group (no. 122) and contains the same M₅L₆ cluster mentioned above ([Figure 1c](#)). Consequently, the total framework of **TMOF** was isorecticular to those **dia**-MOFs^{13a–e} and now with 3-fold interpenetration ([Figure S2](#)). In comparison, the second MOF, formulated as [(CH₃)₂NH₂][Zn₈(tz)₆(TDC)₃]_{0.5}(TDC)_{1.5}·*x*solvents (**TPMOF-1**), crystallizes in the hexagonal space group $P6/mcc$ (no. 192) and exhibits a 3D framework with a distinct network topology. The reaction conditions for yielding **TMOF** and **TPMOF-1** differed only subtly; the key factor was the sequence of ligand addition. For **TMOF**, H₂TDC was added after the reaction of Zn(II) ions and Htz, thereby allowing the construction of the tetrahedral pentanuclear cluster {Zn₅(tz)₆}. By contrast, to prepare **TPMOF-1**, H₂TDC and

Htz were simultaneously added, thus allowing their coordination competition, which prompted the isolation of a novel type of building block {Zn₄(tz)₃} with a triangular frusta shape and further bridged by three TDC^{2–} moieties to initially form a trigonal-prismatic {Zn₈(tz)₆(TDC)₃}.

The most interesting structural feature of **TPMOF-1** is the trigonal-prismatic {Zn₈(tz)₆(TDC)₃}, which can be considered as a double SBU shaped as a triply bound triangular frusta ([Figures 1d](#) and [S3](#)). The aforementioned singly truncated tetrahedral geometric node again emerged, and the asymmetric unit contained two kinds of Zn(II) ions ([Figure S4](#)), one deprotonated tz[–] ligand, and two kinds of TDC^{2–} linkers: TDC1 and TDC2 ([Figure S5](#)). Zn1 was coordinated by three oxygen atoms from three different TDC1 fragments and three nitrogen atoms from three distinct tz[–] ligands, thereby demonstrating a distorted octahedral geometry, while Zn2 exhibited a four-coordinated geometry surrounded by two carboxyl-O atoms from TDC1 and TDC2 fragments, as well as two nitrogen atoms from two tz[–] ligands. One Zn1 and three Zn2 ions were associated by three μ₃-tz[–] to generate a

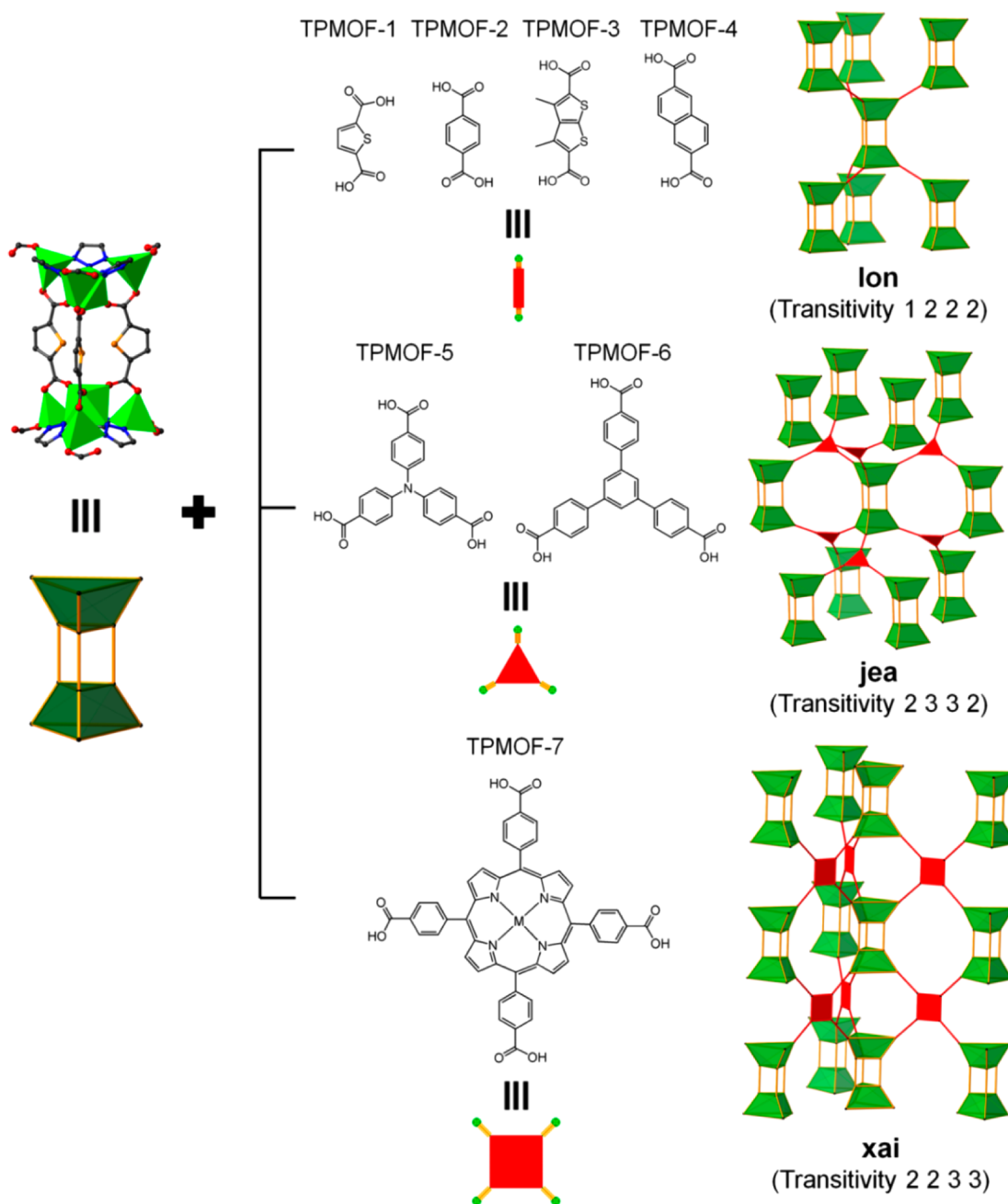


Figure 2. Reticular synthesis of a **TPMOF-*n*** family based on the triply bound triangular frusta SBU $\{Zn_8(tz)_6(TDC)_3\}$ connected with ditopic, tritopic, or tetratopic organic ligands to yield three types of decorated nets. The RCSR symbols and transitivity of corresponding basic (i.e., undecorated) nets are marked.

tetranuclear cluster $\{Zn_4(tz)_3\}$, further bound by three TDC1 fragments to yield the double SBU $\{Zn_8(tz)_6(TDC)_3\}$ with an unusual triply linked triangular frusta geometry.^{13h} Such a double SBU is further connected with adjacent ones by way of six TDC2 fragments, which aid in accomplishing the 3D architecture.

From a topological standpoint, if each tetranuclear $\{Zn_4(tz)_3\}$ SBU is considered to be a 4-connected node and the TDC²⁻ fragment deemed a ditopic linker, then **TPMOF-1** can be described as the lonsdaleite (**lon**) net (Figure 1b), which is rarely observed in MOFs and related crystalline materials.^{1a,10e,14c,21} The voids in a single framework allow another identical network to penetrate therein, thus giving a 2-fold interpenetrating array, but there are still 1D open channels

parallel to the *c* axis. The overall anionic framework shows a free volume of 68.1% based on PLATON calculations.²² The anionic framework of **TPMOF-1** was balanced by $[(CH_3)_2NH_2]^+$ cations, which was formed through the well-established decarbonylation of DMF upon heating around or over 100 °C.^{23a,b} This phenomenon was commonly encountered in the literature.^{23c–f}

Derivation and Decoration of Nets with Trigonal Prisms. In the reticular design of MOFs, it is generally preferred to consider underlying nets with minimal transitivity, that is, the simplest, most symmetrical nets given the local geometry of the building units.⁹ The cases of **dia** and **lon** nets built from tetrahedral 4-connected nodes are ideal examples of this principle;^{1a} though energetically very close, **dia** and **lon**

topologies indeed differ in symmetry and regularity, as measured by transitivity for **dia** shows transitivity 1 1 1 1, whereas **lon** shows transitivity 1 2 2 2.^{9,24} At the same time, **dia** net is most commonly observed in MOFs with tetrahedral nodes, whereas MOFs or related networks with nets augmented or derived from **lon** topology are incredibly rare.^{2d,14c,21}

On the basis of that geometric principle, O’Keeffe et al. enumerated hundreds of 3-periodic nets that could serve as blueprints (i.e., default structures) for MOF construction, thus giving rise to the Reticular Chemistry Structure Resource (RCSR) database.^{2f} It was identified that, for trigonal-prismatic SBUs, the **acs**, **sit**, and **stp** nets are candidates for corresponding MOFs constructed from ditopic, tritopic, and tetratopic linkers, respectively (Scheme 1).¹⁶ The three nets are all found to possess minimal transitivity, and notably, the edge-transitive (3,6)-connected net with trigonal-prismatic node was incompatible with 3-periodicity; therefore, at least two types of edge are needed to link trigonal prisms and triangles in order to form a 3-periodic structure (hence, transitivity 2 2 3 2 for **sit**).^{16c} In practice, **acs**, **sit**, and **stp** nets have been found in MOF-235/236,^{17a,b} MOF-39,^{17c} and tp-PMBB-1-stp-1,^{14a} respectively. The SBUs therein are chemically distinct and no isorecticular series has been reported, thus suggesting that the geometrical designing route for this system remains incomplete.

Subsequently, by way of enumeration, new nets were derived from existing ones in RCSR by splitting the nodes (Scheme 1a).^{9b,16c} As a result, **jea** and **xai** were obtained in the RCSR database by splitting a trigonal prism into a pair of eclipsed tetrahedra in a way with minimal transitivity from **sit** and **stp**, respectively (Scheme 1c,d).²⁵ Interestingly, subject to a similar splitting operation, **acs** becomes **lon** (Scheme 1b), which has nonminimal transitivity. The question then becomes why it emerges and how isorecticular series of such a nondefault structure in real MOFs can be implemented.

It has been conceptualized that, to access the reticular synthesis of nondefault topologies such as **lon**, it is necessary to deconstruct the structure into more elaborate units that express geometric features unique to the structure’s realization.^{1a} The discovery of a double SBU in **TPMOF-1** shaped as a triply linked triangular frusta is crucial for realizing the decorated **lon** net (Figures 1d and 2). In this case, decoration is achieved by retaining the triply bound geometry²⁶ through three TDC²⁻ linkers to enforce the eclipsed conformation, which constitutes a significant local structural feature in decorated **lon** topology. By contrast, each two {Zn₃(tz)₆} units are connected by only one TDC²⁻ linker in **TMOF**, meaning that the staggered conformation is preferred, subject to the minimal transitivity principle, and the underlying net is decorated **dia** (Figure 1c). Another interesting observation of a triply linked (by linear 4,4'-biphenyl-dicarboxyl) triangular frusta SBU was documented;^{13h} however, the framework of the as-synthesized compound adopts the **dia** topology. The result suggests that the shorter length and angular coordination vector of the TDC²⁻ linker may be particularly important in enforcing the eclipsed conformation in the final structure.

Rational Reticular Synthesis of the TPMOF-*n* Family. In the **lon**-MOF **TPMOF-1**, since the two types of TDC²⁻ linkers are topologically independent, it is possible to differentiate them within and beyond the SBU for **lon**, such independence is intrinsic, given its 1 2 2 2 transitivity (i.e., with two kinds of edges).^{9,24} With that in mind, we designed and synthesized an isorecticular series of MOFs, **TPMOF-2** to **-4**, by varying the

lengths of the ditopic carboxylate ligands between the double SBUs (Figure 2).

By introducing another type of extendable ditopic ligand, such as H₂BDC (1,4-benzenedicarboxylic acid), H₂DMTDC (3,4-dimethylthieno[2,3-*b*]thiophene-2,5-dicarboxylic acid), or H₂NDC (2,6-naphthalenedicarboxylic acid) into the four-component system, three isorecticular decorated **lon**-MOFs were produced: **TPMOF-2** ([{(CH₃)₂NH₂]₂[Zn₈(tz)₆(TDC)₃](BDC)₃·*xsolvents*), **TPMOF-3** ([{(CH₃)₂NH₂]₂[Zn₈(tz)₆(TDC)₃](DMTDC)₃·*xsolvents*), and **TPMOF-4** ([{(CH₃)₂NH₂]₂[Zn₈(tz)₆(TDC)₃](NDC)₃·*xsolvents*). X-ray crystallographic analysis reveals that all of them become crystallized in the trigonal space group *P* $\bar{3}$ c1 (no. 165). Their frameworks are composed of two kinds of Zn(II) cations (Figures S6–S8), deprotonated tz⁻, TDC²⁻ and different ditopic moieties (BDC²⁻, DMTDC²⁻, and NDC²⁻, respectively). As in **TPMOF-1**, the double SBU {Zn₈(tz)₆(TDC)₃}, derived from triply bound triangular frusta SBU {Zn₄(tz)₃}, was reproduced in their frameworks. As expected, these {Zn₈(tz)₆(TDC)₃} units were further connected by BDC²⁻, DMTDC²⁻, or NDC²⁻ linkers to yield the **acs** topology (Figure 3). On the other

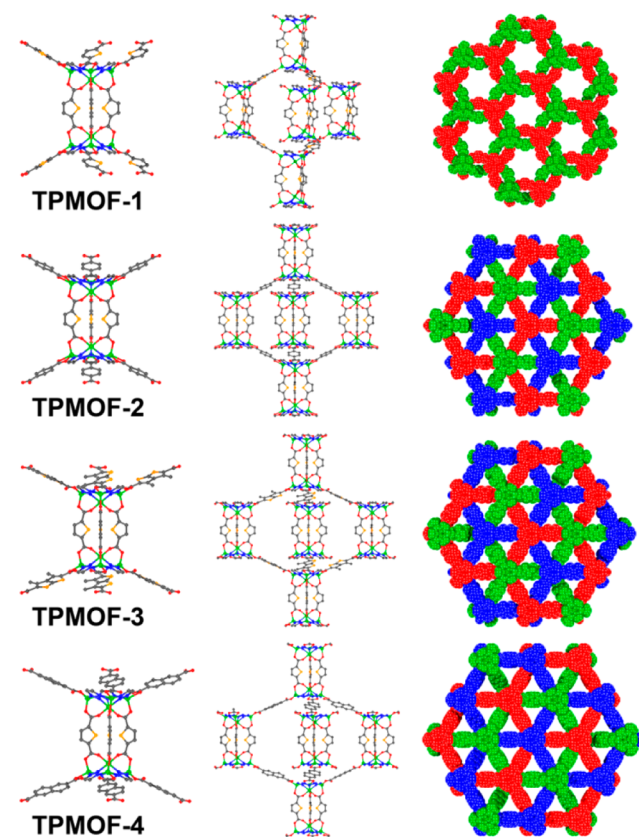


Figure 3. Comparison of **TPMOF-1** to **-4**. (Left) Outer connection modes of the double SBU {Zn₈(tz)₆(TDC)₃}. (Middle) Inter-SBU connection showing voids in between. (Right) Two- or 3-fold interpenetrating 3D frameworks (each shown in a different color).

hand, **TPMOF-2** to **-4** possess the decorated **lon** topology if the double SBU {Zn₈(tz)₆(TDC)₃} was considered as two 4-connected nodes. In addition, **TPMOF-2** to **-4** exhibit 3-fold interpenetration due to enlarged voids by way of ligand extension. The 1D channels are parallel to the *c* axis, which gives rise to free volumes of 61.2%, 67.4%, and 70.1% for

TPMOF-2, -3, and -4, respectively, based on PLATON calculations.²²

Since derived nets **jea** and **xai**—both have minimal transitivity—with tritopic and tetratopic linkers, respectively, have also been predicted in the RCSR database,²⁵ we continued our exploration by introducing tritopic and tetratopic carboxylate ligands. In practice, two types of MOFs, **TPMOF-5** and **TPMOF-6** (Figure 2), were readily synthesized. By replacing the linear linkers with tritopic carboxylic acids tris(4-carboxyphenyl)amine (H_3TCA) or benzene tribenzoate (H_3BTB), two new products, **TPMOF-5** ($[(CH_3)_2NH_2]_2[Zn_8(tz)_6(TDC)_3](TCA)_2 \cdot x\text{solvents}]$) and **TPMOF-6** ($[(CH_3)_2NH_2]_2[Zn_8(tz)_6(TDC)_3](BTB)_2 \cdot x\text{solvents}]$), were yielded (Figures S9 and S10), both crystallized in the monoclinic space group $C2/m$ (no. 12). Again, the double SBU $\{Zn_8(tz)_6(TDC)_3\}$ were reproduced and extended by the tritopic linkers to yield the **sit** net. Furthermore, if the double SBU $\{Zn_8(tz)_6(TDC)_3\}$ is considered as two 4-connected nodes, they adopt the decorated **jea** topology (Scheme 1) that has never been reported in MOF chemistry before. The accessible free volumes were calculated by PLATON to be 70.8% and 77.6% for **TPMOF-5** and **TPMOF-6**,²² respectively, despite the 2-fold interpenetration that reduced the channel voids running along the *a* axis (Figures 4 and S11).

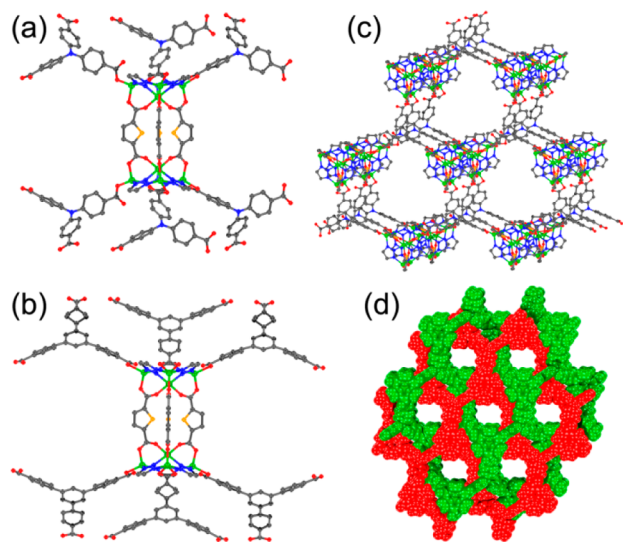


Figure 4. Outer connection modes of the double SBU $\{Zn_8(tz)_6(TDC)_3\}$ in (a) **TPMOF-5** and (b) **TPMOF-6**. (c) View of the 1D channel structure in the single framework of **TPMOF-5** and (d) 2-fold interpenetrating 3D framework of **TPMOF-5**.

The **TPMOF-7(Zn)** with a tetratopic linker, Zn-TCPP (TCPP = tetrakis(4-carboxyphenyl)porphyrin), was formulated to be $[(CH_3)_2NH_2]_2[Zn_8(tz)_6(TDC)_3](Zn-TCPP)_{1.5} \cdot x\text{solvents}]$ and crystallized in the orthorhombic space group $Cmca$ (no. 64). It consists of four crystallographically unique Zn(II) ions—Zn1 with distorted octahedral geometry and Zn2, Zn3, and Zn4 with distorted tetrahedral geometry (Figure S12)—three deprotonated tz^- fragments, 3/2 deprotonated TDC^{2-} moieties, and 3/4 square-planar Zn-TCPP fragments. The double SBU $\{Zn_8(tz)_6(TDC)_3\}$ was further linked by the Zn-TCPP fragments to produce the **stp** topology (Figure 5). After close inspection of the architecture, **TPMOF-7(Zn)** also possesses the decorated **xai** topology if the double SBU was regarded as two 4-connected nodes (Scheme 1), which is rarely

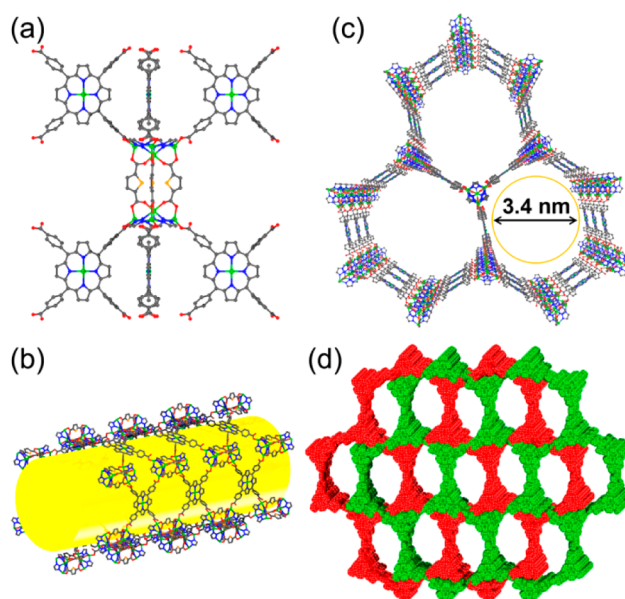


Figure 5. Structure of **TPMOF-7**: (a) outer connection mode of the double SBU $\{Zn_8(tz)_6(TDC)_3\}$, (b) top and (c) side views of the 1D channel in the single framework, and (d) the 2-fold interpenetrating 3D framework.

observed in MOF chemistry. A single 3D framework of **TPMOF-7(Zn)** exhibits a channel running along the *a* axis, with an average diameter of approximately 3.4 nm. The framework-accessible free volume was calculated to be 79.7% using PLATON,²² despite 2-fold interpenetration. Such voids are potentially accessible for catalytic reactions.^{10d} When Fe-TCPP was used instead of Zn-TCPP, **TPMOF-7(Fe)** possessing the same underlying framework was obtained under similar reaction conditions (Figure S13), as confirmed by the subsequent XRPD pattern. The successful construction of **TPMOF-7(Fe)** with different active metal sites in the tetratopic metalloporphyrinic ligand paves the way for application in heterogeneous biomimetic catalysis.

It should be noted that the decorated nets shown in Figure 2 for the **TPMOF-*n*** family differ from the augmented nets (i.e., a special kind of decorated net) **lon-a**, **jea-a**, and **xai-a** (Scheme 1) collected in the RCSR database, since the triply bound mode is specified in the spirit of reticular deconstruction and reversal design. Interestingly, the **sit** net is intrinsically polar and tends to occur intergrown with nets of opposite polarity to yield a nonpolar structure.^{16c} This trait is indeed apparent in **TPMOF-5** and **TPMOF-6**, which exhibit 2-fold interpenetration with slightly different translational vectors (Figure S14b,c). The doubly catenated nets of **TPMOF-1** and **TPMOF-7** are also presented for comparison (Figure S14a,d), which reveals that the double SBUs therein also tend to orient in a polar way in a single net, especially in the catenated decorated **lon** net.

Porosity and Catalytic Performance. Powder X-ray diffraction (PXRD) patterns were collected to examine the phase purity of the bulk products of **TMOF** and **TPMOF-*n*** family. The PXRD patterns of synthesized samples matched well with those simulated ones from single-crystal diffraction analyses (Figures S15–S22), thus indicating the phase purity of the as-synthesized samples.

To assess the porosity and the architectural stability of **TPMOF-7**, nitrogen adsorption–desorption isotherm measurements were carried out at 77 K. Initially, we performed the

activation procedures to ensure that the pores were activated and free of guest molecules. **TPMOF-7(Fe)** was subjected to solvent exchange followed by evacuation and treated with supercritical carbon dioxide, to obtain porous samples named **TPMOF-7(Fe)a**. As shown in Figure S23, the nitrogen adsorption isotherm of **TPMOF-7(Fe)a** at 77 K exhibited type I isotherm. The maximum N_2 adsorption amount was $291.4 \text{ cm}^3 \cdot \text{g}^{-1}$ at standard temperature and pressure (STP) and the Brunauer–Emmett–Teller (BET) surface area was calculated to be $879 \text{ m}^2 \cdot \text{g}^{-1}$. The architectural stability and permanent porosity of **TPMOF-7(Fe)** was confirmed by N_2 adsorption experiments.

The enzymatic catalytic process exhibits great potential in chemical manufacturing; however, engineering enzymes is severely hindered by their low operational stability. The architectural stability and pore structure based on the Fe–TCPP fragment prompted us to evaluate the biocatalytic performance of **TPMOF-7(Fe)**. The oxidation reaction of 2,2'-azino(3-ethylbenzothiazoline)-6-sulfonate (ABTS) to $\text{ABTS}^{+\bullet}$ is routinely used to evaluate the peroxidase activity of porphyrin catalysts (Figure 6a).^{12f,26} In this context, the catalytic activity of

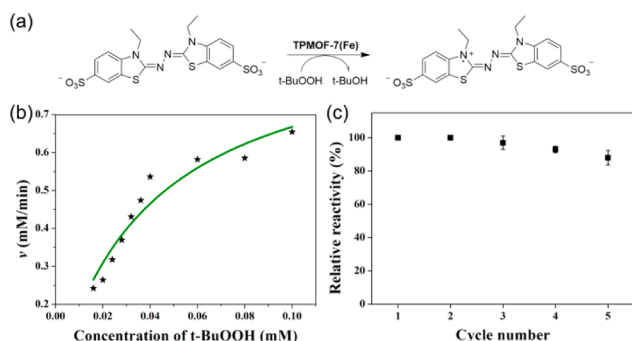


Figure 6. Oxidation reaction of ABTS catalyzed by **TPMOF-7(Fe)**: (a) the oxidation reaction scheme for ABTS, which is oxidized to $\text{ABTS}^{+\bullet}$ by **TPMOF-7(Fe)** in the presence of *t*-BuOOH; (b) Michaelis–Menten curve fit for the ABTS oxidation catalyzed by **TPMOF-7(Fe)**; (c) the oxidation reaction with **TPMOF-7(Fe)** at different cycles.

TPMOF-7(Fe) was evaluated by way of an electron transfer reaction. The reaction process was monitored at 403 nm with a particular range of *tert*-butyl hydroperoxide (*t*-BuOOH) concentration by UV–vis spectroscopy, as consistent with typical Michaelis–Menten kinetics (Figure 6b). The turnover number k_{cat} represents the maximum number of substrate molecules converted to product per catalyst molecule per unit time, thus giving a direct measure of catalytic activity. The Michaelis–Menten constant K_m is often associated with the affinity of the catalyst for the substrate, from which the catalytic efficiency (k_{cat}/K_m) can be obtained using a Michaelis–Menten curve fit. For this reaction, the derived k_{cat} of **TPMOF-7(Fe)** catalyst shows a value of 3.87 min^{-1} . **TPMOF-7(Fe)** exhibits peroxidase-like catalytic activity, better than that of the reported CHF-1 (0.45 min^{-1} , Table S2).^{26b} The derived (K_m) value of **TPMOF-7(Fe)** (0.041 mM) is less than that of Cyt c (48.3 mM), MP-11 (3.28 mM), and HRP (0.15 mM).^{12f,26b} Additionally, the catalytic efficiency of **TPMOF-7(Fe)** is approximately $9.44 \times 10^4 \text{ M}^{-1} \cdot \text{min}^{-1}$, which is greater than that of CHF-1 ($2.06 \times 10^4 \text{ M}^{-1} \cdot \text{min}^{-1}$), Cyt c ($1.36 \times 10^3 \text{ M}^{-1} \cdot \text{min}^{-1}$), and MP-11 ($2.445 \times 10^4 \text{ M}^{-1} \cdot \text{min}^{-1}$).^{12f,26b} Such an excellent catalytic electron transfer can be attributed to the high

density of the heme active centers in **TPMOF-7(Fe)**, which perhaps facilitates the affinity for the substrate ABTS.

The heterogeneous catalyst was recovered for a further test of ABTS oxidation at different cycles, with the initial rates examined in order to evaluate its recyclability. With increasingly larger cycle numbers, the catalytic activity of **TPMOF-7(Fe)** gradually decreased, and with the fifth cycle, it continued to retain approximately 88% of its initial activity (Figure 6c). Furthermore, the PXRD pattern indicates that the network of **TPMOF-7(Fe)** was retained after the catalytic reaction (Figure S22).

CONCLUSIONS

In this work, efforts toward the topological design and reticular synthesis of MOFs are explained from both theoretical and experimental perspectives. On the one hand, with the derivation and decoration of nets with trigonal-prismatic nodes, new blueprints (e.g., **jea** derived from **sit** and **xai** derived from **stp**) for MOF construction existed a priori, whereas **lon** can be similarly derived from **acs**, despite its nonminimal transitivity. On the other hand, the experimental realization of a reproducible double SBU, triply bound triangular frusta $\{\text{Zn}_8(\text{tz})_6(\text{TDC})_3\}$, connecting with ditopic, tritopic, and tetratopic organic linkers, afforded the decorated **lon**, **jea**, and **xai** topologies, when the double SBU was considered as two 4-connected nodes. With such a marriage of chemistry and mathematics, **TPMOF-*n*** family can be synthesized in a rationally designable way. The targeted MOFs exhibit progressively increased pore sizes from **TPMOF-1** to **-7**, thereby eventually warranting highly active biomimetic catalysis within Fe–porphyrin-based **TPMOF-7(Fe)**. The heightened complexity encoded in such a systematic route endues new opportunities in searching made-to-order MOFs pertaining to energy and environmental demands and beyond.

EXPERIMENTAL SECTION

Preparation of TMOF. $\text{Zn}(\text{NO}_3)_2 \cdot 6\text{H}_2\text{O}$ (0.089 g, 0.30 mmol) was added to a DMF solution (6 mL) containing Htz (0.021 g, 0.30 mmol) and the mixture stirred for 30 min. Next, H_2TDC (0.017 g, 0.10 mmol) was added to above mixture, and then the resulting mixture was heated at 100°C for 48 h. Colorless block crystals were collected after it was cooled to room temperature and dried in air (yield 81%, based on H_2TDC). IR (Figure S24, KBr pellets, ν/cm^{-1}): 3448 (m), 3141 (m), 2928 (m), 1656 (s), 1580 (m), 1526 (m), 1384 (s), 1254 (w), 1188 (m), 1105 (s), 1023 (w), 979 (m), 820 (m), 770 (m), 719 (w), 665 (m), 513 (m).

Preparation of TPMOF-1 to -7. For **TPMOF-1**: $\text{Zn}(\text{NO}_3)_2 \cdot 6\text{H}_2\text{O}$ (0.148 g, 0.50 mmol) was added to a DMF solution (6 mL) containing a mixture of Htz (0.021 g, 0.30 mmol) and H_2TDC (0.052 g, 0.30 mmol) and the mixture stirred for 20 min. Then, the resulting mixture was heated at 100°C for 48 h. Colorless block crystals were harvested after the mixture was cooled to room temperature and dried in air (yield 83%, based on H_2TDC). IR (Figure S25a, KBr pellets, ν/cm^{-1}): 3391 (m), 1662 (m), 1571 (s), 1460 (m), 1359 (s), 1191 (m), 1121 (m), 1029 (w), 976 (m), 811 (m), 770 (s), 681 (w), 554 (m), 523 (m).

For **TPMOF-2 to -4**: $\text{Zn}(\text{NO}_3)_2 \cdot 6\text{H}_2\text{O}$ (0.148 g, 0.50 mmol) was added to a DMF solution (6 mL) containing a mixture of Htz (0.021 g, 0.30 mmol) and H_2TDC (0.026 g, 0.15 mmol) and then the solution stirred for 20 min. Next, H_2BDC (0.025 g, 0.15 mmol) was added to the mixture with stirring for another 20 min. The resulting mixture was heated at 100°C for 48 h. Colorless block crystals were collected after the mixture was cooled to room temperature and dried in air (yield 74%, based on H_2BDC). IR (Figure S25b, KBr pellets, ν/cm^{-1}): 3441 (m), 2928 (m), 1669 (s), 1574 (s), 1390 (s), 1254 (m), 1191 (m), 1124 (m), 1099 (m), 1020 (w), 982 (m), 808 (m), 770 (m), 751 (m),

659 (m), 554 (w), 523 (m). With the substitution of H₂BDC with H₂DMTDC and H₂NDC, colorless block crystals **TPMOF-3** and **-4** were obtained. IR for **TPMOF-3** (Figure S25c, KBr pellets, ν/cm^{-1}): 3443 (m), 2930 (m), 1665 (s), 1574 (s), 1527 (m), 1500 (s), 1460 (m), 1438 (m), 1389 (s), 1254 (m), 1193 (w), 1121 (m), 1100 (s), 1061 (w), 1022 (w), 981 (w), 831 (m), 809 (m), 786 (m), 770 (m), 663 (m), 617 (w), 556 (w), 524 (m), 420 (w). IR for **TPMOF-4** (Figure S25d, KBr pellets, ν/cm^{-1}): 3429 (s), 1664 (s), 1573 (s), 1391 (s), 1252 (w), 1193 (m), 1111 (m), 1029 (w), 982 (w), 922 (w), 802 (m), 774 (m), 664 (w), 557 (w), 522 (m), 475 (m).

For **TPMOF-5** and **-6**: Zn(NO₃)₂·6H₂O (0.148 g, 0.50 mmol) was added to a DMF solution (6 mL) containing a mixture of Htz (0.021 g, 0.30 mmol) and H₂TDC (0.026 g, 0.15 mmol). Then, H₃TCA (0.038 g, 0.10 mmol) was added to the mixture with stirring for 20 min and the resulting mixture was heated at 100 °C for 72 h. Yellow block crystals were collected after the mixture was cooled to room temperature and dried in air (yield 77%, based on H₃TCA). IR (Figure S26a, KBr pellets, ν/cm^{-1}): 3436 (s), 1661 (s), 1592 (s), 1387 (s), 1315 (m), 1274 (m), 1180 (m), 1111 (m), 982 (w), 850 (w), 818 (w), 777 (m), 673 (m), 522 (m). Colorless block crystals of **TPMOF-6** were isolated by the same method as the synthesis of **TPMOF-5**, but using H₃BTB in substitution for H₃TCA. IR (Figure S26b, KBr pellets, ν/cm^{-1}): 3430 (m), 1661 (s), 1573 (s), 1391 (s), 1256 (w), 1190 (w), 1105 (m), 1017 (m), 979 (w), 863 (w), 812 (m), 775 (m), 668 (w), 526 (w).

For **TPMOF-7(Zn)** and **TPMOF-7(Fe)**: Zn(NO₃)₂·6H₂O (0.148 g, 0.50 mmol) was added to a DMA solution (6 mL) containing a mixture of Htz (0.021 g, 0.30 mmol) and H₂TDC (0.026 g, 0.15 mmol) with stirring for 20 min. Then, Zn–TCPP (0.068 g, 0.08 mmol) was added to the mixture, this stirred for another 20 min, and the resulting mixture was heated at 100 °C for 72 h. Purple block crystals were harvested after the mixture was cooled to room temperature and dried in air (yield 65%, based on H₂TDC). IR (Figure S27a, KBr pellets, ν/cm^{-1}): 3427 (m), 2935 (m), 1634 (s), 1571 (s), 1504 (m), 1390 (s), 1260 (m), 1188 (m), 1118 (m), 1010 (m), 804 (w), 773 (m), 713 (w), 592 (m), 523 (w), 478 (w). **TPMOF-7(Fe)** was synthesized by employing the same synthetic condition as that of **TPMOF-7(Zn)** except for Fe–TCPP instead of Zn–TCPP. IR (Figure S27b, KBr pellets, ν/cm^{-1}): 3427 (m), 2935 (m), 1631 (s), 1574 (s), 1526 (m), 1393 (s), 1260 (m), 1188 (m), 1118 (s), 1004 (m), 808 (w), 773 (m), 713 (w), 592 (m), 523 (w), 478 (w).

Topological Analysis. The coordinates of the derived 3-periodic nets and their intrinsic symmetries (space group and transitivity) were determined by the computer code Systre (available via gavrog.org).^{2c} Detailed geometric information on all nets mentioned in the text can be found in the RCSR database (available via rcsr.net).^{2f}

■ ASSOCIATED CONTENT

Supporting Information

The Supporting Information is available free of charge on the ACS Publications website at DOI: [10.1021/jacs.6b01093](https://doi.org/10.1021/jacs.6b01093).

Experimental details, figures, tables (PDF)

Crystallographic data for TMOF and TPMOF-1–7 (CIF)

■ AUTHOR INFORMATION

Corresponding Authors

*yqlan@njnu.edu.cn

*zhou@chem.tamu.edu

Notes

The authors declare no competing financial interest.

■ ACKNOWLEDGMENTS

The synthetic and structural studies of this research was supported by the Center for Gas Separations Relevant to Clean Energy Technologies, an Energy Frontier Research Center funded by the U.S. Department of Energy, Office of Science,

Office of Basic Energy Sciences under Award Number DESC0001015. The authors also acknowledge the financial supports of the National Natural Science Foundation of China (Nos. 21371099, 21401021, and 21471080), China Postdoctoral Science Foundation (No. 2015T80284), the NSF of Jiangsu Province of China (No. BK20130043), the Priority Academic Program Development of Jiangsu Higher Education Institutions, the Foundation of Jiangsu Collaborative Innovation Center of Biomedical Functional Materials, and the Science and Technology Development Planning of Jilin Province (Nos. 20140520089JH and 20140203006GX). We thank Dr. He-Xiang Deng (Wuhan University, China) for gas adsorption study treated with supercritical carbon dioxide. We also thank Prof. Michael O'Keeffe (Arizona State University, United States) for his helpful structural comments on TPMOF-*n* family.

■ REFERENCES

- (1) (a) Yaghi, O. M.; O'Keeffe, M.; Ockwig, N. W.; Chae, H. K.; Eddaoudi, M.; Kim, J. *Nature* **2003**, *423*, 705. (b) Kitagawa, S.; Kitaura, R.; Noro, S. *Angew. Chem., Int. Ed.* **2004**, *43*, 2334. (c) Férey, G. *Chem. Soc. Rev.* **2008**, *37*, 191. (d) Batten, S. R.; Champness, N. R.; Chen, X.-M.; Garcia-Martinez, J.; Kitagawa, S.; Öhrström, L.; O'Keeffe, M.; Suh, M. P.; Reedijk, J. *Pure Appl. Chem.* **2013**, *85*, 1715. (e) Furukawa, H.; Cordova, K. E.; O'Keeffe, M.; Yaghi, O. M. *Science* **2013**, *341*, 1230444. (f) Furukawa, H.; Müller, U.; Yaghi, O. M. *Angew. Chem., Int. Ed.* **2015**, *54*, 3417.
- (2) (a) Delgado-Friedrichs, O.; Dress, A. W. M.; Huson, D. H.; Klinowski, J. A.; Mackay, L. *Nature* **1999**, *400*, 644. (b) O'Keeffe, M.; Eddaoudi, M.; Li, H.; Reineke, T.; Yaghi, O. M. *J. Solid State Chem.* **2000**, *152*, 3. (c) Delgado-Friedrichs, O.; O'Keeffe, M. *Acta Crystallogr., Sect. A: Found. Crystallogr.* **2003**, *59*, 351. (d) Ockwig, N. W.; Delgado-Friedrichs, O.; O'Keeffe, M.; Yaghi, O. M. *Acc. Chem. Res.* **2005**, *38*, 176. (e) Delgado-Friedrichs, O.; O'Keeffe, M.; Yaghi, O. M. *Phys. Chem. Chem. Phys.* **2007**, *9*, 1035. (f) O'Keeffe, M.; Peskov, M. A.; Ramsden, S. J.; Yaghi, O. M. *Acc. Chem. Res.* **2008**, *41*, 1782.
- (3) (a) Li, J.-R.; Kuppler, R. J.; Zhou, H.-C. *Chem. Soc. Rev.* **2009**, *38*, 1477. (b) Sumida, K.; Rogow, D. L.; Mason, J. A.; McDonald, T. M.; Bloch, E. D.; Herm, Z. R.; Bae, T.-H.; Long, J. R. *Chem. Rev.* **2012**, *112*, 724. (c) Li, J.-R.; Sculley, J.; Zhou, H.-C. *Chem. Rev.* **2012**, *112*, 869. (d) He, Y.; Zhou, W.; Qian, G.; Chen, B. *Chem. Soc. Rev.* **2014**, *43*, 5657.
- (4) (a) Kreno, L. E.; Leong, K.; Farha, O. K.; Allendorf, M.; Van Deyne, R. P.; Hupp, J. T. *Chem. Rev.* **2012**, *112*, 1105. (b) Hu, Z.; Deibert, B. J.; Li, J. *Chem. Soc. Rev.* **2014**, *43*, 5815.
- (5) (a) Lee, J. Y.; Farha, O. M.; Roberts, J.; Scheidt, K. A.; Nguyen, S. T.; Hupp, J. T. *Chem. Soc. Rev.* **2009**, *38*, 1450. (b) Corma, A.; García, H.; Llabrés i Xamena, F. X. *Chem. Rev.* **2010**, *110*, 4606. (c) Du, D.-Y.; Qin, J.-S.; Li, S.-L.; Su, Z.-M.; Lan, Y.-Q. *Chem. Soc. Rev.* **2014**, *43*, 4615. (d) Zhang, T.; Lin, W. *Chem. Soc. Rev.* **2014**, *43*, 5982. (e) Liu, J.; Chen, L.; Cui, H.; Zhang, J.; Zhang, L.; Su, C.-Y. *Chem. Soc. Rev.* **2014**, *43*, 6011.
- (6) (a) Imaz, I.; Rubio-Martínez, M.; An, J.; Solé-Font, I.; Rosi, N. L.; Maspocho, D. *Chem. Commun.* **2011**, *47*, 7287. (b) McKinlay, A. C.; Morris, R. E.; Horcajada, P.; Férey, G.; Gref, R.; Couvreur, P.; Serre, C. *Angew. Chem., Int. Ed.* **2010**, *49*, 6260. (c) Zhang, M.; Gu, Z.-Y.; Bosch, M.; Perry, Z.; Zhou, H.-C. *Coord. Chem. Rev.* **2015**, *293–294*, 327. (d) Cai, H.; Li, M.; Lin, X.-R.; Chen, W.; Chen, G.-H.; Huang, X.-C.; Li, D. *Angew. Chem., Int. Ed.* **2015**, *54*, 10454.
- (7) Four themed issues of reviews on MOFs are available: (a) Themed issue: Metal–organic frameworks, Long, J. R., Yaghi, O. M., Eds; *Chem. Soc. Rev.* **2009**, Vol. 38, pp 1201–1508. (b) Special issue: Metal–Organic Frameworks, Zhou, H.-C., Long, J. R., Yaghi, O. M., Eds; *Chem. Rev.* **2012**, Vol. 112, pp 673–1268. (c) Themed issue: Metal–organic frameworks, Zhou, H.-C., Kitagawa, S., Eds; *Chem. Soc. Rev.* **2014**, Vol. 43, pp 5403–6176. (d) Chemistry and Applications of

Metal Organic Frameworks, Levason, B., Bradshaw, D., Eds.; *Coord. Chem. Rev.* **2016**, Vol. 307, pp 105–424.

- (8) (a) Yaghi, O. M.; Li, H.; Davis, C.; Richardson, D.; Groy, T. L. *Acc. Chem. Res.* **1998**, 31, 474. (b) Batten, S. R.; Robson, R. *Angew. Chem., Int. Ed.* **1998**, 37, 1460. (c) Eddaoudi, M.; Moler, D. B.; Li, H.; Chen, B.; Reineke, T. M.; O'Keeffe, M.; Yaghi, O. M. *Acc. Chem. Res.* **2001**, 34, 319. (d) Deng, H.; Doonan, C. J.; Furukawa, H.; Ferreira, R. B.; Towne, J.; Knobler, C. B.; Wang, B.; Yaghi, O. M. *Science* **2010**, 327, 846. (e) Bunck, D. N.; Dichtel, W. R. *Chem. - Eur. J.* **2013**, 19, 818. (f) Guillermin, V.; Kim, D.; Eubank, J. F.; Luebke, R.; Liu, X.; Adil, K.; Lah, M. S.; Eddaoudi, M. *Chem. Soc. Rev.* **2014**, 43, 6141. (g) Blatov, V. A.; Shevchenko, A. P.; Proserpio, D. M. *Cryst. Growth Des.* **2014**, 14, 3576. (h) Tu, B.; Pang, Q.; Ning, E.; Yan, W.; Qi, Y.; Wu, D.; Li, Q. *J. Am. Chem. Soc.* **2015**, 137, 13456.
- (9) (a) O'Keeffe, M.; Yaghi, O. M. *Chem. Rev.* **2012**, 112, 675. (b) Li, M.; Li, D.; O'Keeffe, M.; Yaghi, O. M. *Chem. Rev.* **2014**, 114, 1343.
- (10) (a) Tranchemontagne, D. J.; Mendoza-Cortés, J. L.; O'Keeffe, M.; Yaghi, O. M. *Chem. Soc. Rev.* **2009**, 38, 1257. (b) Zhang, Y.-B.; Zhou, H.-L.; Lin, R.-B.; Zhang, C.; Lin, J.-B.; Zhang, J.-P.; Chen, X.-M. *Nat. Commun.* **2012**, 3, 642. (c) Zhao, X.; Bu, X.; Wu, T.; Zheng, S.-T.; Wang, L.; Feng, P. *Nat. Commun.* **2013**, 4, 2344. (d) Guillermin, V.; Weseliński, L. J.; Belmabkhout, Y.; Cairns, A. J.; D'Elia, V.; Wojtas, L.; Adil, K.; Eddaoudi, M. *Nat. Chem.* **2014**, 6, 673. (e) Schoedel, A.; Zaworotko, M. J. *Chem. Sci.* **2014**, 5, 1269.
- (11) (a) Lu, W.; Wei, Z.; Gu, Z.-Y.; Liu, T.-F.; Park, J.; Park, J.; Tian, J.; Zhang, M.; Zhang, Q.; Gentle, T., III; Bosch, M.; Zhou, H.-C. *Chem. Soc. Rev.* **2014**, 43, 5561. (b) He, Y.; Li, B.; O'Keeffe, M.; Chen, B. *Chem. Soc. Rev.* **2014**, 43, 5618. (c) Gao, W.-Y.; Chrzanowski, M.; Ma, S. *Chem. Soc. Rev.* **2014**, 43, 5841. (d) Yan, H.; Yang, S.; Blake, A. J.; Schröder, M. *Acc. Chem. Res.* **2014**, 47, 296. (e) Wang, T. C.; Bury, W.; Gómez-Gualdrón, D. A.; Vermeulen, N. A.; Mondloch, J. E.; Deria, P.; Zhang, K.; Moghadam, P. Z.; Sarjeant, A. A.; Snurr, R. Q.; Stoddart, J. F.; Hupp, J. T.; Farha, O. K. *J. Am. Chem. Soc.* **2015**, 137, 3585. (f) Liu, T.-F.; Feng, D.; Chen, Y.-P.; Zou, L.; Bosch, M.; Yuan, S.; Wei, Z.; Fordham, S.; Wang, K.; Zhou, H.-C. *J. Am. Chem. Soc.* **2015**, 137, 413. (g) Feng, D.; Wang, K.; Wei, Z.; Chen, Y.-P.; Simon, C. M.; Arvapally, R. K.; Martin, R. L.; Bosch, M.; Liu, T.-F.; Fordham, S.; Yuan, D.; Omary, M. A.; Haranczyk, M.; Smit, B.; Zhou, H.-C. *Nat. Commun.* **2014**, 5, 5723.
- (12) (a) Chui, S. S.-Y.; Lo, S. M.-F.; Charmant, J. P. H.; Orpen, A. G.; Williams, I. D. *Science* **1999**, 283, 1148. (b) Férey, G.; Serre, C.; Mellot-Draznieks, C.; Millange, F.; Surblé, S.; Dutour, J.; Margiolaki, I. *Angew. Chem., Int. Ed.* **2004**, 43, 6296. (c) Férey, G.; Mellot-Draznieks, C.; Serre, C.; Millange, F.; Dutour, J.; Surblé, S.; Margiolaki, I. *Science* **2005**, 309, 2040. (d) Li, H.; Eddaoudi, M.; O'Keeffe, M.; Yaghi, O. M. *Nature* **1999**, 402, 276. (e) Cavka, J. H.; Jakobsen, S.; Olsbye, U.; Guillou, N.; Lamberti, C.; Bordiga, S.; Lillerud, K. P. *J. Am. Chem. Soc.* **2008**, 130, 13850. (f) Feng, D.; Liu, T.-F.; Su, J.; Bosch, M.; Wei, Z.; Wan, W.; Yuan, D.; Chen, Y.-P.; Wang, X.; Wang, K.; Lian, X.; Gu, Z.-Y.; Park, J.; Zou, X.; Zhou, H.-C. *Nat. Commun.* **2015**, 6, 5979.
- (13) (a) Bai, Y.-L.; Tao, J.; Huang, R.-B.; Zheng, L.-S. *Angew. Chem., Int. Ed.* **2008**, 47, 5344. (b) Wang, X.-L.; Qin, C.; Wu, S.-X.; Shao, K.-Z.; Lan, Y.-Q.; Wang, S.; Zhu, D.-X.; Su, Z.-M.; Wang, E.-B. *Angew. Chem., Int. Ed.* **2009**, 48, 5291. (c) Zhang, Z.; Xiang, S.; Chen, Y.-S.; Ma, S.; Lee, Y.; Phely-Bobin, T.; Chen, B. *Inorg. Chem.* **2010**, 49, 8444. (d) Lan, Y.-Q.; Li, S.-L.; Jiang, H.-L.; Xu, Q. *Chem. - Eur. J.* **2012**, 18, 8076. (e) Gándara, F.; Uribe-Romo, F. J.; Britt, D. K.; Furukawa, H.; Lei, L.; Cheng, R.; Duan, X.; O'Keeffe, M.; Yaghi, O. M. *Chem. - Eur. J.* **2012**, 18, 10595. (f) Qin, J.-S.; Zhang, S.-R.; Du, D.-Y.; Shen, P.; Bao, S.-J.; Lan, Y.-Q.; Su, Z.-M. *Chem. - Eur. J.* **2014**, 20, 5625. (g) Qin, Y.-Y.; Zhang, J.; Li, Z.-J.; Zhang, L.; Cao, X.-Y.; Yao, Y.-G. *Chem. Commun.* **2008**, 2532. (h) Li, Y.-W.; Wang, L.-F.; He, K.-H.; Chen, Q.; Bu, X.-H. *Dalton Trans.* **2011**, 40, 10319.
- (14) (a) Schoedel, A.; Wojtas, L.; Kelley, S. P.; Rogers, R. D.; Eddaoudi, M.; Zaworotko, M. J. *Angew. Chem., Int. Ed.* **2011**, 50, 11421. (b) Schoedel, A.; Cairns, A. J.; Belmabkhout, Y.; Wojtas, L.; Mohamed, M.; Zhang, Z.; Proserpio, D. M.; Eddaoudi, M.; Zaworotko, M. J. *Angew. Chem., Int. Ed.* **2013**, 52, 2902. (c) Schoedel, A.; Boyette, W.; Wojtas, L.; Eddaoudi, M.; Zaworotko, M. J. *J. Am. Chem. Soc.* **2013**, 135, 14016.
- (15) (a) Perry, J. J., IV; Kravtsov, V. C.; McManus, G. J.; Zaworotko, M. J. *J. Am. Chem. Soc.* **2007**, 129, 10076. (b) Yuan, D.; Zhao, D.; Sun, D.; Zhou, H.-C. *Angew. Chem., Int. Ed.* **2010**, 49, 5357.
- (16) (a) Delgado-Friedrichs, O.; O'Keeffe, M.; Yaghi, O. M. *Acta Crystallogr., Sect. A: Found. Crystallogr.* **2003**, 59, 515. (b) Delgado-Friedrichs, O.; O'Keeffe, M.; Yaghi, O. M. *Acta Crystallogr., Sect. A: Found. Crystallogr.* **2006**, 62, 350. (c) O'Keeffe, M. *APL Mater.* **2014**, 2, 124106.
- (17) (a) Serre, C.; Millange, F.; Surblé, S.; Férey, G. *Angew. Chem., Int. Ed.* **2004**, 43, 6286. (b) Sudik, A. C.; Côté, A. P.; Yaghi, O. M. *Inorg. Chem.* **2005**, 44, 2998. (c) Kim, J.; Chen, B.; Reineke, T. M.; Li, H.; Eddaoudi, M.; Moler, D. B.; O'Keeffe, M.; Yaghi, O. M. *J. Am. Chem. Soc.* **2001**, 123, 8239. (d) Wang, K.; Feng, D.; Liu, T.-F.; Su, J.; Yuan, S.; Chen, Y.-P.; Bosch, M.; Zou, X.; Zhou, H.-C. *J. Am. Chem. Soc.* **2014**, 136, 13983.
- (18) (a) Koh, K.; Wong-Foy, A. G.; Matzger, A. J. *Angew. Chem., Int. Ed.* **2008**, 47, 677. (b) Koh, K.; Wong-Foy, A. G.; Matzger, A. J. *J. Am. Chem. Soc.* **2009**, 131, 4184. (c) Koh, K.; Wong-Foy, A. G.; Matzger, A. J. *J. Am. Chem. Soc.* **2010**, 132, 15005. (d) Klein, N.; Senkovska, I.; Gedrich, K.; Stoeck, U.; Henschel, A.; Mueller, U.; Kaskel, S. *Angew. Chem., Int. Ed.* **2009**, 48, 9954. (e) Furukawa, H.; Ko, N.; Go, Y. B.; Aratani, N.; Choi, S. B.; Choi, E.; Yazaydin, A. Ö.; Snurr, R. Q.; O'Keeffe, M.; Kim, J.; Yaghi, O. M. *Science* **2010**, 329, 424. (f) He, W.-W.; Yang, G.-S.; Tang, Y.-J.; Li, S.-L.; Zhang, S.-R.; Su, Z.-M.; Lan, Y.-Q. *Chem. - Eur. J.* **2015**, 21, 9784.
- (19) (a) Liu, L.; Konstas, K.; Hill, M. R.; Telfer, S. G. *J. Am. Chem. Soc.* **2013**, 135, 17731. (b) Liu, L.; Telfer, S. G. *J. Am. Chem. Soc.* **2015**, 137, 3901. (c) Dutta, A.; Wong-Foy, A. G.; Matzger, A. J. *Chem. Sci.* **2014**, 5, 3729.
- (20) Feng, D.; Wang, K.; Su, J.; Liu, T.-F.; Park, J.; Wei, Z.; Bosch, M.; Yakovenko, A.; Zou, X.; Zhou, H.-C. *Angew. Chem., Int. Ed.* **2015**, 54, 149.
- (21) (a) Zou, Y.; Yu, C.; Li, Y.; Lah, M. S. *CrystEngComm* **2012**, 14, 7174. (b) Cui, P.; Wu, J.; Zhao, X.; Sun, D.; Zhang, L.; Guo, J.; Sun, D. *Cryst. Growth Des.* **2011**, 11, 5182. (c) Sreenivasulu, B.; Vittal, J. J. *Cryst. Growth Des.* **2003**, 3, 635. (d) Kitazawa, T.; Kikuyama, T.; Takeda, M.; Iwamoto, T. *J. Chem. Soc., Dalton Trans.* **1995**, 3715. (e) Kim, H.; Sun, Y.; Kim, Y.; Kajiwara, T.; Yamashita, M.; Kim, K. *CrystEngComm* **2011**, 13, 2197. (f) Chun, H.; Bak, W.; Hong, K.; Moon, D. *Cryst. Growth Des.* **2014**, 14, 1998. (g) Patil, K. M.; Dickinson, M. E.; Tremlett, T.; Moratti, S. C.; Hanton, L. R. *Cryst. Growth Des.* **2016**, 16, 1038.
- (22) Spek, A. L. *J. Appl. Crystallogr.* **2003**, 36, 7.
- (23) (a) Perrin, D. D.; Armarego, W. L. F. *Purification of Laboratory Chemicals*, 3rd ed.; Pergamon: Oxford, 1988. (b) Wan, Y.; Alterman, M.; Larhed, M.; Hallberg, A. *J. Org. Chem.* **2002**, 67, 6232. (c) Sudik, A. C.; Millward, A. R.; Ockwig, N. W.; Côté, A. P.; Kim, J.; Yaghi, O. M. *J. Am. Chem. Soc.* **2005**, 127, 7110. (d) Sudik, A. C.; Côté, A. P.; Wong-Foy, A. G.; O'Keeffe, M.; Yaghi, O. M. *Angew. Chem., Int. Ed.* **2006**, 45, 2528. (e) Zheng, S.-T.; Bu, J. T.; Li, Y.; Wu, T.; Zuo, F.; Feng, P.; Bu, X. *J. Am. Chem. Soc.* **2010**, 132, 17062. (f) Neofotistou, E.; Malliakas, C. D.; Trikalitis, P. N. *CrystEngComm* **2010**, 12, 1034. (g) Zheng, S.-T.; Wu, T.; Irfanoglu, B.; Zuo, F.; Feng, P.; Bu, X. *Angew. Chem., Int. Ed.* **2011**, 50, 8034. (h) Zheng, S.-T.; Wu, T.; Zuo, F.; Chou, C.; Feng, P.; Bu, X. *J. Am. Chem. Soc.* **2012**, 134, 1934. (i) Xue, D.-X.; Cairns, A. J.; Belmabkhout, Y.; Wojtas, L.; Liu, Y.; Alkordi, M. H.; Eddaoudi, M. *J. Am. Chem. Soc.* **2013**, 135, 7660.
- (24) Transitivity $p \ q \ r \ s$ means topologically there are p kinds of vertices, q kinds of edges, r kinds of faces, and s kinds of tiles, which has been used as a measure of "regularity" of a net.
- (25) See the Web Page in RCSR: <http://rcsr.net/nets/jea> and <http://rcsr.net/nets/xai>.
- (26) (a) Chen, Y.; Hoang, T.; Ma, S. *Inorg. Chem.* **2012**, 51, 12600. (b) Wang, X.-S.; Chrzanowski, M.; Yuan, D.; Sweeting, B. S.; Ma, S. *Chem. Mater.* **2014**, 26, 1639.